ASSOCIATE PROFESSOR JOANNA KIRMAN (Orcid ID : 0000-0002-4802-7048)
ASSOCIATE PROFESSOR THOMAS PROFT (Orcid ID : 0000-0002-9275-5042)

Article type : Original Article

Intranasal immunisation with Ag85B peptide 25 displayed on *Lactococcus lactis* using the PilVax platform induces antigen-specific B- and T-cell responses

Running title: Immunisation with Ag85B peptide 25 using PilVax

Samuel Blanchett[1,#,Ŧ], Catherine JY Tsai[1,2,Ŧ], Sarah Sandford[3], Jacelyn MS Loh[1,2], Lucy Huang[3], Joanna R Kirman[2,3*], Thomas Proft[1,2*]

[1]Department of Molecular Medicine and Pathology, School of Medical Sciences, The University of Auckland, Auckland, New Zealand.

[2]Maurice Wilkins Centre for Biomolecular Discoveries, The University of Auckland, Auckland, New Zealand.

[3]Department of Microbiology & Immunology, University of Otago, Dunedin, New Zealand.

#present address: Division of Infection & Immunity, Faculty of Medical Sciences, University College London, U.K.*Joint senior authors. Correspondence to Thomas Proft (t.proft@auckland.ac.nz) and Joanna Kirman (jo.kirman@otago.ac.nz)

Ŧ authors contributed equally.

Keywords: *Mycobacterium tuberculosis*; TB; PilVax; vaccine; peptide

Abstract

Mycobacterium tuberculosis (*Mtb*) remains a global epidemic despite the widespread use of BCG. Consequently, novel vaccines are required to facilitate a reduction in *Mtb* morbidity and mortality.

PilVax is a peptide delivery strategy for the generation of highly specific mucosal immune responses and is based on the food-grade bacterium *Lactococcus lactis* that is used to express selected peptides engineered within the *Streptococcus pyogenes* M1T1 pilus, allowing for peptide amplification, stabilisation, and enhanced immunogenicity. In the present study, the dominant T cell epitope from the *Mtb* protein Ag85B was genetically engineered into the pilus backbone subunit and expressed on the surface of *L. lactis*. Western blot and flow cytometry confirmed formation of pilus containing the peptide DNA sequence. B cell responses in intranasally vaccinated mice were analysed by ELISA while T cell responses were analysed by flow cytometry. Serum titres of peptide specific IgG and IgA were detected, confirming vaccination produced antibodies against the cognate peptide. Peptide-specific IgA was also detected across several mucosal sites sampled. Peptide-specific $CD4^+$ T cells were detected at levels similar to those of mice immunised with BCG. PilVax immunisation resulted in an unexpected increase in the numbers of $CD3^+CD4^-CD8^-$ (double negative, DN) T cells in the lungs of vaccinated mice. Analysis of cytokine production following stimulation with the cognate peptide showed the major cytokine producing cells to be $CD4^+$ T cells and DN T cells. This study provides insight into the antibody and peptide specific cellular immune responses generated by PilVax vaccination and demonstrates the suitability of this vaccine for conducting a protection study.

Introduction

Before the recent SARS-Cov2 virus pandemic, *Mycobacterium tuberculosis* (*Mtb*), the causative agent of tuberculosis (TB), was the leading cause of death by a single infectious agent, resulting in 1.5 million deaths in 2018 [1]. The World Health Organisation estimated that in 2018 1.23 billion people had latent TB infections and there were 10 million new cases of active TB [1]. The increasing prevalence of multi-drug resistant TB strains and extensively-drug resistant *Mtb* strains threatens the ability to control TB through antibiotic use [1, 2]. Moreover, due to the lengthy 6–9 months of antibiotic treatment required for drug-

susceptible TB, direct treatment costs combined with productivity loss is estimated by the Centres for Disease Control to be US$49 000 per case in the USA [3].

The only licenced TB vaccine is live, attenuated *Mycobacterium bovis*, known as *Bacille Calmette–Guérin* (BCG) [4]. Developed in the early 20th century, BCG vaccination has had varying degrees of success in preventing disease (0–80% efficacy) [5]. Although BCG is most effective in children, it is unreliable at preventing pulmonary TB in adult populations where 85% of the TB burden lies [6, 7]. The poorly characterised mechanism of protection achieved through BCG vaccination in children, and the lack of natural sterilising immunity following *Mtb* infection have hindered the identification of a correlate of protection, further complicating *Mtb* vaccine development. While there is no definitive correlate of protection, TB vaccines candidates have been postulated to elicit protection through mechanisms such as the development of peptide specific T_{CM} (central memory) and T_{RM} (resident memory) cells [8], and induction of T cells that simultaneously produce TNFα, IFN-γ, IL-2 and IL-17 and combinations thereof[9–11].

Antibodies may also contribute to protection against *Mtb* [12]. Highlighting their importance, the protective effects of BCG are diminished in B cell deficient mice where the T cell response was also reduced [13]. Contradictory findings from studies that have investigated the role of antibody in protection against TB have led to uncertainty about their role. This may be due to differences in antigen specificity and isotype, which can affect antibody functionality in TB. Further research is required to elucidate the precise role antibodies facilitate in the immune response to this pathogen.

Despite the lack of a clear immune correlate of protection, there are now several dozen novel TB vaccines in the pre-clinical and clinical testing pipeline. Ag85B is the target of several pre-clinical vaccine candidates (reviewed in Karbalaei Zadeh Babaki *et al.* [15]) and a component of the subunit vaccine, H56:IC3. Antigen-specific protection has been demonstrated in phase 2b clinical trials of that vaccine [16]. Ag85B is a mycolyl transferase that is involved with cell wall synthesis and is hyper-

conserved amongst mycobacterial strains including BCG [14]. Therefore Ag85B, along with other immunogenic secreted TB proteins, is a useful target antigen for novel TB vaccines.

Similar to the current BCG vaccine, most novel TB vaccines in the clinical trial pipeline rely on intramuscular (i.m.) or intradermal (i.d.) administration. Since *Mtb* infects the host via contact with the mucosal surfaces in the respiratory tract, protection could be enhanced by targeting a vaccine to the site where the pathogen is first encountered. Intranasal administration (i.n.) of BCG or H56 improved control over a subsequent aerosol *Mtb* challenge compared to subcutaneous (s.c.) administration [17]. Furthermore, i.n. vaccines enhance ease of vaccine delivery by offering needle free administration [18].

Novel i.n. approaches such as a PilVax have potential to be exploited for *Mtb* vaccines. PilVax is a peptide delivery strategy utilising the pilus of the exclusive human pathogen *Streptococcus pyogenes* (Group A Streptococcus, GAS) expressed in the food-grade bacterium, *Lactococcus lactis* [19]. The GAS pilus is a hair-like, peritrichous projection from the surface of the cell that functions primarily in adhesion and biofilm formation [20]. The pilus consists of a long oligomeric fibre made up of covalently linked backbone pilin (Spy0128 in serotype M1T1 strains) and a tip pilin that functions as an adhesin (collagen-binding protein, Cpa). Some GAS pili, like the M1T1 pilus also contain an anchor protein that attaches the pilus to the bacterial cell wall [21–23]. Heterologous expression of the pilus is possible in *L. lactis* and it was demonstrated that peptides of interest can be engineered into the backbone pilin with minimal effect on pilus expression [19]. Insertion of a peptide within this construct has several advantages: (1) prevention of peptide degradation, (2) removes the need for expensive chemical coupling to carrier proteins (3) peptide multimerisation along the pilus fibre increasing peptide immunogenicity, and (4) the absence of potentially toxic adjuvants.

I.n. delivery of a prototype PilVax vaccine in mice elicited a strong mucosal and peptide specific antibody response to the model ovalbumin $Ova_{324–339}$ peptide [19]. More recently, PilVax was used as a vaccine carrier for the $D3_{(22–33)}$ peptide from the fibronectin-binding protein A of *Staphylococcus aureus* and stimulated peptide-specific systemic and mucosal responses in immunised mice [24]. Here we present a

study using the dominant T cell epitope $Ag85B_{240–254}$ (peptide 25) [25] from the highly immunogenic Ag85B protein (residues 240–254 in the mature protein and residues 280–294 in the precursor protein) for expression in PilVax. $Ag85B_{240–254}$ is a major T_h1 cell epitope in I-A(b) mice which can drive development of $CD4^+$ T_h1 cells that produce IFN-γ and TNF-α, and protect against subsequent infection with *Mtb* [25, 26]. We demonstrate that peptide specific $CD4^+$ T cells and antibodies are induced by i.n. vaccination with a *L. lactis* PilM1-$Ag85B_{240–254}$ construct.

Results

The $Ag85B_{240–254}$ peptide from *Mtb* can be expressed in PilVax

Previous characterisation of the pilus backbone protein, Spy0128, revealed peptides can be inserted into specific variable loop regions of the protein without affecting the assembly of the pilus when expressed in *L. lactis* [19]. The $Ag85B_{240–254}$ peptide (FQDAYNAAGGHNAVF) was genetically engineered into the βE/βF loop region of the pilus backbone protein replacing most of the loop residues. The complete modified pilus structure was expressed on the surface of *L. lactis.* Expression and polymerisation of the pilus fibre was confirmed by Western blot analysis using Spy0128-specific antibodies and is evident by the characteristic high molecular weight laddering pattern observed (Figure 1**a**). Laddering occurs due to the covalent assembly of the pilin monomers that generate pilus fibres of variable length. Flow cytometry was used to quantify the amount of pili expressed on the *L. lactis* cell surface and the MFI of the PilM1-$Ag85B_{240–254}$ construct was approximately 10-times lower than the MFI of the *L. lactis* PilM1 construct (M1/T1 pilus without inserted peptide) indicating pilus assembly was reduced because of peptide insertion (Figure 1**b**). However, as expression of the pili in *L. lactis* is under the control of a strong constitutive promotor we concluded that the amount of peptide presented on the bacterial cell surface might be sufficient to trigger specific immune responses.

Intranasal vaccination induces peptide-specific antibodies

To establish immunogenicity of PilM1-Ag85B$_{240\text{-}254}$, vaccination was delivered i.n. using low-volume bacterial suspensions (1 x 10^8 cfu 5 μL^{-1}) in 12 doses. We have previously shown that this immunisation regimen triggers good antibody responses, including mucosal IgA[19]. *L. lactis* expressing PilM1-Ova$_{324–339}$ or PilM1 were included as controls. Two weeks following the final boost, serum, bronchoalveolar lavage (BAL) fluid, saliva, nasal and faecal samples were obtained and analysed for Spy0128 and peptide-specific antibodies by ELISA. The serum anti-Spy0128 titres were analysed to ensure reliable and consistent administration of the bacterial suspensions. Immunisation with *L. lactis* PilM1-Ag85B$_{240–254}$ and PilM1- Ova $_{324–339}$ resulted in comparable average anti-Spy0128 titres, similar to previously reported titres for PilM1- Ova $_{324–339.}$ [19] (Figure 2**a**), despite the reduced expression of Spy0128 pilins on the bacterial cell surface of the PilM1-Ag85B$_{240–254}$ construct (Figure 1**b**). Serum IgG and IgA titers against the cognate peptides were also comparable between the different constructs. As expected from a systemic site, peptide-specific IgG titres were approximately 1.5 $\log_{10}$ higher than IgA titres (Figure 2**b**). However, there were differences in IgA titres at some local sites. In BAL fluid, Ova-specific IgA titers were approximately 10-fold higher than Ag85B-specific IgA responses, whereas approximately 10-fold higher Ag85B-specific IgA levels were detected in saliva compared to Ova-specific IgA, although IgA titers were generally low (< 10^3). IgA against Ova was also observed in fecal samples whereas IgA levels against Ag85B were barely detectable (Figure 2**c**). Despite the intranasal delivery route, no Ova or Ag85B-specific IgAs were detected in nasal washes (Figure 2**c**).

Once immunogenicity was established with PilM1-Ag85B$_{240–254}$, a subsequent study was performed vaccinating mice intranasally with *L. lactis* expressing PilM1-Ag85B$_{240–254}$ in a larger volume (2 x 10^7 cfu/40 µl) over three doses in total to ensure delivery to the lower respiratory tract, the primary site of TB infection [5, 27] with the goal of inducing Ag85B-specific T cell responses in the lung. Antibody responses were compared to mice immunised s.c. with BCG. Anti-Ag85B$_{240–254}$ IgG was detected in serum at levels

comparable to control mice injected s.c. with BCG, but at titres approximately 10-fold lower than observed in mice vaccinated with *L. lactis* PilM1-Ag85B$_{240–254}$ using the low volume dose (Figure 2**d**). No detectable anti-Ag85B$_{240–254}$ IgA responses were observed in the serum after lower respiratory tract delivery of *L. lactis* PilM1-Ag85B$_{240–254}$ nor were anti-Ag85B$_{240–254}$ IgA responses detected after subcutaneous BCG vaccination.

To ensure that the specific Ag85B antibodies raised against *L. lactis* PilM1-Ag85B$_{240–254}$ are not only able to recognise the Ag85B peptide, but also the complete Ag85B protein, we tested commercially obtained recombinant Ag85B in an ELISA. Mouse anti- Ag85B$_{240–254}$ but not preimmune-serum reacted against whole Ag85B (Figure 2**e**).

Intranasal vaccination induces peptide specific CD4$^+$ T cells

To assess T cell responses, mice were immunised intranasally with *L. lactis* expressing PilM1-Ag85B$_{240–254}$ in the larger volume (2 x 10^7 cfu 40 μL^{-1}) over three doses in total to ensure delivery to the lower respiratory tract.

Three weeks after the final booster vaccination, pulmonary CD4$^+$ lymphocytes specific for the Ag85B$_{240–254}$ peptide were analysed by flow cytometry using MHC Class II tetramers. Significant expansion of Ag85B$_{240–254}$-specific T cells were detected in both the *L. lactis* PilM1-Ag85B$_{240–254}$ and BCG vaccinated groups (Figure 3) compared to control from *L. lactis* PilM1-vaccinated mice. The mean proportion of CD4$^+$ T cells specific for the Ag85B$_{240–254}$ peptide was 1.86% in the *L. lactis* PilM1-Ag85B$_{240–254}$ vaccinated mice and slightly higher at 2.17% in the BCG vaccinated mice (Figure 3**b**), but this was not statistically significant. The mean number of CD4$^+$ lymphocytes in the lung that were specific for the Ag85B$_{240–254}$ peptide were also similar between the *L. lactis* PilM1-Ag85B$_{240–254}$- and BCG-vaccinated groups at 1.3 x 10^3 and 4.8 x 10^3, respectively (Figure 3**b**). The number of CD4$^+$ T cells detected using the control hCLIP tetramer was similar to those from *L. lactis* PilM1-vaccinated mice.

CD4$^+$ T cells identified are primarily T_{RM}

CD4$^+$ Ag85B$_{240–254}$ peptide specific cells were further characterised by measuring cell surface expression of CD44, CD69 and CD62L to identify populations of central memory-like T cells (T_{CM}), resident memory-like T cells (T_{RM}), and effector memory-like T cells (T_{EM}). CD44 was used to identify antigen experienced cells, while CD62L is upregulated in T_{CM} cells, and low in T_{EM} and T_{RM} cells. CD69 expression was used to identify T_{RM} cells in conjunction with other markers. Most Ag85B$_{240–254}$ peptide specific CD4$^+$ T cells identified in the lungs of *L. lactis* PilM1-Ag85B$_{240–254}$ and BCG vaccinated mice were T_{RM}-like (64.4% and 73.8% respectively) followed by T_{EM}-like (29.8% and 16.2%). Only small populations of T_{CM}-like cells (less than 5%) were detected (Figure 3**c**).

Double negative (DN) T cells are produced in PilVax vaccinated mice

Pulmonary lymphocytes from mice vaccinated with the large dose regimen (lower respiratory tract delivery) were stimulated with cognate peptide *ex vivo* to analyse the cytokine response. While analysing this data, a large population of CD4$^-$CD8$^-$CD3$^+$ (DN) T cells was observed in mice vaccinated with *L. lactis* PilM1-Ag85B$_{240–254}$ and *L. lactis* PilM1 (37% and 39%) compared to BCG vaccinated mice (10%) (Figure 4**a**, **b**). A CD4$^+$/CD8$^+$ T cell ratio of 2.0 is expected in healthy individuals and indeed is seen in BCG vaccinated mice (ratio of 2.2). The CD4$^+$/CD8$^+$ T cell ratio was disturbed in *L. lactis* PilM1-Ag85B$_{240–254}$ and *L. lactis* PilM1 vaccinated mice (ratios of 1.40 and 1.39, respectively), and DN T cells were the largest cell type present. The lack of this cell population in s.c. vaccinated BCG mice suggests that the expansion of these cells is due to either (1) the repeated i.n. administration of the *L. lactis* constructs, or (2) an effect of the live *L. lactis* or the pilus proteins entering the lungs during vaccination.

Predominant cytokine production is a result of CD4$^+$ T cells producing IFN-γ and IL-17

Following *ex vivo* stimulation with cognate peptide, the cytokine production of pulmonary lymphocytes was identified through intracellular cytokine staining (Figure 5). Boolean gating was used to identify cells

producing a single cytokine, or combinations of IL-2, IL-17, TNF-α, and IFN-γ. In *L. lactis* PilM1-Ag85B$_{240–254}$ vaccinated mice, 1.23% CD4$^+$ cells were producing IFN-γ, compared to 2.73% of CD4$^+$ cells from BCG vaccinated mice. However, only in *L. lactis* PilM1- Ag85B$_{240–254}$ vaccinated mice was small proportion (0.5%) of IFN-γ and IL-17 producing CD4$^+$ cells detected (Figure 6**a**). Cytokine production by CD8$^+$ T cells was not expected, as the Ag85B$_{240–254}$ peptide is presented on MHC class II. As such, the only observable cytokine production in CD8$^+$ T cells was from BCG-vaccinated mice where 1.05% of cells were producing IFN-γ (Figure 6**b**). Analysis of DN T cells from *L. lactis* PilM1-Ag85B$_{240–254}$– and BCG-vaccinated mice showed a broader range of cytokine production compared to CD4$^+$ and CD8$^+$ T cells (Figure 6**c**). In BCG-vaccinated mice the mean percentage of DN T cells producing IFN-γ (2.43%), IL-2 (2.37%), TNF-α (0.53%) and IL-17 (1.99%) was higher than observed in *L. lactis* PilM1-Ag85B$_{240–254}$ vaccinated mice, where most cytokine-producing cells were making IL-17 (1.5%) followed by IFN-γ (0.74%), IL-2 (0.71%), and TNF-α (0.42%). Although the amount of cytokine produced was not measured, the absolute number of DN T cells producing each cytokine, or a combination (with the exception of IL-2) was higher in *L. lactis* PilM1-Ag85B$_{240–254}$ vaccinated mice than BCG vaccinated mice (Table 1). Notably, apart from the CD4$^+$ T cells producing both IFN-γ and IL-17 following stimulation with cognate peptide in *L. lactis* PilM1-Ag85B$_{240–254}$ vaccinated mice, most cells produced only a single cytokine.

Discussion

PilVax is a peptide presentation platform that utilises the extended surface-exposed pilus structure of the GAS M1T1 serotype (PilM1) expressed on the food-grade bacterium *L. lactis*. Integration of the peptide results in stabilisation and multimerisation of the peptide on the surface of *L. lactis*. PilM1 was chosen as the protein structures of the three proteins that make up the pilus fibre have been solved [21, 22, 28]. *L. lactis* has been used to generate many experimental vaccines due to their immunostimulatory effects [29].The bacteria do not colonise animals or humans and are quickly cleared by the host immune response. We

have shown that the PilVax platform can be used to present the *Mtb* Ag85B$_{240–254}$ peptide (peptide 25) stably as part of the GAS pilus structure on the surface of the *L. lactis*. Immunisation of mice with *L. lactis* PilM1-Ag85B$_{240–254}$ elicited the expansion of antigen-specific CD4$^+$ T cells and production of peptide specific antibodies. This is the first study that shows the capability of the PilVax platform to generate both T and B cell responses in a disease context. We have also shown evidence that the dominant T cell epitope of Ag85B can act as a B cell epitope, which has not been reported before.

Despite the whole Ag85B protein being using in clinical trial vaccines, such as the H56 vaccine where it fused to ESAT-6, the protection seen in these trials have been attributed to cells specific for the Ag85B $_{240–254}$ peptide[32]. However, there are currently no peptide vaccines for TB in clinical trials. Here we utilised the known antigen core of the protein and inserted the Ag85B$_{240–254}$ peptide into the Spy0128 pilin for use in PilVax. Peptide insertion did not prevent pilin polymerisation as high-molecular laddering was observed in Western blots but shorter and reduced expression of pili were detected. Nevertheless, immunisation of mice with *L. lactis* PilM1 Ag85B$_{240–254}$ generated similar levels of serum anti-Spy0128 antibodies compared to *L. lactis* PilM1 Ova$_{324–339}$ immunised mice suggesting that the length of the pili and therefore the amount of surface-presented peptide was sufficient for an adequate immune response. Indeed, we observed a strong systemic and mucosal antibody response to the Ag85B$_{240–254}$ peptide with comparable titres to the Ova$_{324–339}$ peptide. This was surprising as Ag85B$_{240–254}$ is a known T cell epitope and this is the first report demonstrating that Ag85B$_{240–254}$ is also able to function as a B cell epitope. The benefit of generating such mucosal antibodies, which are only weakly induced by s.c., i.d., and i.m. vaccines, is that pathogen-specific IgA at mucosal sites may prevent colonisation by steric hindrance. This has been seen with other pathogens such as influenza [33], *E. coli* [34], and *Helicobacter pylori* [35]. IgA has been shown to be important for *Mtb* protection and the presence of anti-Ag85B IgA in the respiratory tract could aid in preventing colonisation [36].

There were small differences in the IgA responses between the two peptides; Ag85B $_{240–254}$ generated a higher antibody titre in saliva compared to Ova$_{324–339}$ whereas an opposite response was seen in BAL fluid. Surprisingly, despite the i.n. delivery, no antigen specific antibodies were detected in the nasal wash. Other vaccines targeting the nasal mucosa through i.n. vaccination, such as those in trial for influenza, have been able to elicit nasal IgA and indeed correlate the presence of these antibodies with protection. Such trials have used inactivated virus, which may result in signalling through different pathways than live bacteria due to the involvement of different TLRs [37]. However, since *Mtb* largely colonises the lower respiratory tract, in this instance anti–Ag85B IgA in the BAL fluid may be of more value in preventing *Mtb* colonisation compared to nasal tissue.

Initially mice were vaccinated with a low dose of *L. lactis* PilM1-Ag85B$_{240–254}$ over 12 doses as previously described [19] to assess the initial immunogenicity of *L. lactis* PilM1-Ag85B$_{240–254}$. It was unknown if antibodies would be generated against more than just the model Ova peptide in PilVax. To assess PilVax in an *Mtb* context, the vaccination volume and anaesthesia were adjusted to facilitate lower respiratory tract delivery. Previous works have identified intranasal vaccinations against *Mtb* need to reach the lower respiratory tract (LRT) to achieve an appropriate immune response [5, 27]. Ag85B-specific serum IgG was detectable in both BCG and *L. lactis* PilM1-Ag85B$_{240–254}$ vaccinated groups. This antibody response may be important for opsonisation-induced phagocytosis of *Mtb*, as has been observed with *Mtb* peptidoglycan-specific IgG from BCG vaccinated humans [36]. Using the LRT dosage schedule, the titres of serum anti-Ag85B$_{240–254}$ IgG were lower than when a low volume dose was used. There is potential to increase both IgG and IgA through an additional vaccination boost (unpublished data). Further boosts that result in the presence of serum IgA could be advantageous as there is evidence this class has the potential to mediate protection as passive transfer of anti-*Mtb* α-crystallin IgA has resulted in transient immunity.

Intranasal immunisation with *L. lactis* PilM1-Ag85B$_{240–254}$ delivered to the LRT also generated a significant cellular response. Ag85B$_{240–254}$ peptide-specific CD4$^+$ T cells were found in the lungs in similar numbers to the BCG-vaccinated control mice, and significantly greater than in PilM1 controls. The highest number of Ag85B$_{240–254}$ specific CD4$^+$ T cells observed by Vogelzang *et al.* [30] 18 days following vaccination with the vaccine candidate VPM1002 was 5x10^3, and 10^4 with the H56 vaccine [31]. This was of a similar magnitude to the number of Ag85B$_{240–254}$ specific CD4$^+$ T cells we detected in the lungs of *L. lactis* PilM1-Ag85B$_{240–254}$ vaccinated mice at 12 days after the final vaccination. VPM1002 is a live recombinant BCG strain that was developed to enhance CD8$^+$ T cell activation through the expression of listeriolysin from *Listeria monocytogenes*, while the H56 vaccine is a fusion protein of Ag85B and ESAT-6. With similar numbers of Ag85B specific T cells induced as other vaccines where protection is observed, PilVax could offer further improvements on s.c. BCG vaccination due to the route of administration as mucosal delivery of BCG, and aerosol delivery of H56 vaccination improved the clearance of *Mtb* in challenge studies [38]

In our study, the predominant phenotype of antigen-specific cells in the lungs of both PilVax and BCG immunised mice, was T_{RM} cells with a smaller population of T_{EM} cells and no significant generation of T_{CM} cells. Lung resident T_{RM} cells are a population of cells able to rapidly respond to infection in the pulmonary parenchyma and are implicated in protection against viral pathogens. The role of T_{RM} cells has not been an extensive focus of *Mtb* vaccine research to date. However, populations of this resident cell type are persistent following BCG vaccination and were able to mediate protection against challenge in a study when memory T cells were sequestered in the lymph nodes by treatment with fingolimod [39]. T_{RM} cells have also been implicated in protection against *Mtb* infection in a previous murine study where BCG was delivered to the respiratory mucosa, albeit via intra tracheal (i.t.) delivery [38]. Following this i.t. vaccination a large influx of T_{RM} cells to the lungs was observed that, although not maintained long term, were attributed to the reduction in disease burden when challenged with *Mtb*. A similar phenomenon was

seen by Vogelzang *et al.* [30] who reported an initial short term increase in T_{RM} cells induced by VPM1002 before returning to similar levels invoked by conventional BCG vaccination. Both VPM1002 and H56 vaccines offered superior protection compared with BCG. In a study by Perdomo and colleagues, the T_{RM} cells invoked by i.t. BCG vaccination were able to confer protection in an adoptive transfer model highlighting the potential of *Mtb* specific T_{RM} cells generated from mucosal vaccines [38].

Although present, T_{EM} cells have not typically been associated with protection against *Mtb* due to their lower replicative capacity and shorter life span compared to the other cell types. Despite this, protection induced by the DAR-901 vaccine candidate in human trials is reportedly mediated by cytokine producing T_{EM} cells, further highlighting the complexity and difficulty in identifying a correlate of protection [40].

Interestingly, a large population of $CD4^{-}CD8^{-}$ $CD3^{+}$ T cells was observed in re-stimulated pulmonary lymphocytes isolated from PilVax $Ag85B_{240–254}$ vaccinated mice. These were significantly higher than the $CD4^{-}CD8^{-}$ $CD3^{+}$ T cell population observed after BCG vaccination. Double negative (DN) $CD3^{+}$ T cells have been previously observed following repeated *in vitro* stimulation of pulmonary murine cells with anti-CD3/CD28 beads and during pulmonary *Francisella tularensis* live vaccine strain (LVS) vaccination in mice [41, 42]. The proliferation of DN T cells was absent in i.d. LVS administration implicating the i.n. delivery as the cause of this phenotype. Thus, the repetitive LRT PilVax delivery is likely responsible for the proliferation of this T cell subtype observed in *L. lactis* PilM1-$Ag85B_{240–254}$ and *L. lactis* PilM1 vaccinated mice.

We observed IFN-γ, IL-2 and IL-17 production by DN $CD3^{+}$ T cells after *L. lactis* PilM1-$Ag85B_{240–254}$ vaccination. Production of IFN-γ and IL-17A by DN $CD3^{+}$ T cells was also observed after *F. tularensis* LVS vaccination and this improved *F. tularensis* clearance following infection in a synergistic manner [42]. Since *F. tularensis* is an intracellular pathogen like *Mtb,* this IFN-γ^{+} IL-$17A^{+}$ DN T cell phenotype could also be important for *Mtb* control. However, a definitive cytokine profile that correlates with protection

against *Mtb* has not been identified, with each novel vaccine inducing a different cytokine fingerprint [43]. In DAR-901 clinical trials, where enhanced protection was observed compared to BCG, the amount of cytokine produced was no higher than in BCG vaccination [38]. Alternatively, a marked increase in the number of polyfunctional T cells has been attributed to the protective capacity of some *Mtb* vaccines candidates [9-11, 43].

The evidence presented here suggests further investigation into the protective capacity of PilVax as a vaccine candidate for *Mtb* prevention or treatment is warranted. These findings are significant for *Mtb* vaccine development, firstly, the i.n. mucosal vaccine delivery could be advantageous over other i.m and i.d. vaccines due to direct priming of the mucosal associated lymphoid tissue where infecting *Mtb* first encounters the immune system. Secondly, in a low income setting where TB is most prevalent, i.n. administration of *L. lactis* expressing PilVax constructs affords a needle free, technically non-challenging route of administration. While PilVax has required multiple doses to generate the peptide specific T cells and antibodies seen here, precedence for this exists in a human context where an i.n influenza vaccine requiring multiple boosts with a nasal spray for seroconversion has already been successfully trialled and tolerated in clinical trials [37]. This could be harnessed when targeting PilVax for diseases where the dose is not required to reach the lungs. However, large volume pulmonary vaccines have also been trialled and tolerated in non-human primates suggesting this method of vaccination could be used for PilVax-$Ag85B_{240–254}$ in humans [40].

These findings also provide basis for future work with PilVax and other diseases. Inclusion of multiple epitopes within the Spy0128 monomer could provide a broader specificity of immune responses by targeting either multiple antigens within the same pathogen such as peptides from the highly immunogenic *Mtb* protein ESAT-6, or even multiple pathogens in the same construct. However, the protective capacity of the peptide-specific immune response seen here has yet to be determined and

further investigation is required. The presence of anti-peptide antibodies in the fecal samples might be a result of the highly communicative nature of the MALT and indicate PilVax could also be used to generate mucosal antibodies in the gastrointestinal (GI) tract.

These findings provide promising insights into the potential of PilVax as a peptide delivery strategy for vaccines. The generation of local, and systemic antibodies combined with peptide specific T cells opens up the potential for a PilVax construct to be developed for a variety of diseases providing a cost-effective and efficient vaccine delivery system.

Methods

Bacterial culture

L. lactis MG1363 was grown statically in M17 media (BD Bioscience) supplemented with 0.5% glucose (GM17) at 28°C or on GM17 media supplemented with 1.5% w/v Bacto agar (BD Bioscience, San Jose, CA, USA). *E. coli* DH5α was grown with shaking at 37°C in LB broth (Duchefa Biochemie, Haarlem, Netherlands) supplemented with 0.95% w/v NaCl or LB broth supplemented with 1.5% w/v Bacto agar (BD Bioscience). Antibiotics (Sigma-Aldrich, St. Louis, MO, USA) were added when required: ampicillin (50 μg mL^{-1}, *E. coli*), kanamycin (50 μg mL^{-1}, *E. coli*; 200 μg mL^{-1}, *L. lactis*).

Genetic manipulations

The DNA sequence corresponding to the $Ag85B_{240–254}$ peptide was generated by PCR with overlapping primers (Ag85B.fw CGGATCC CTCGAGTTTCAAGATGCTTATAATGCTG CAGGTGG and Ag85B.rv CGGAATTC CTCGAGAAAAACAGCGTTATGTCCACC TGCAGCATTA) using a Master Cycler Nexus (Eppendorf, Hamburg, Germany). DNA was purified with a QIAquick PCR purification kit (QIAGEN, Hilden, Germany) and digested with *SalI* (New England Biolabs, Ipswich, MA, USA) overnight at 37°C. The reaction was stopped by heat inactivation. The vector for insertion was the pLZ12km2_P23R plasmid. The vector contained the GAS SF370 (serotype M1) pilus operon with an

XhoI site at the βE/βF loop region of the *spy0128* gene sequence (AAK33238) generated as previously described. Prior to ligation with peptide DNA sequences, the vector was digested with *XhoI,* gel purified (QIAquick gel extraction kit, QIAGEN), and dephosphorylated with alkaline phosphatase (Roche). The ligation mixture was transformed into *E. coli* DH5α by heat shock.

DNA sequences were confirmed using ABI Sequencing and Genotyping services at Massey University, Palmerston North, New Zealand. Resulting plasmids were transformed into *L. lactis* strain MG1363 by electroporation at 2100 V, 25 μF, 200 Ω in a 2-mm cuvette using a Gene Pulser Xcell^{TK} (BioRad, Hercules, CA, USA). Expression and assembly of pili on the *L. lactis* cell surface was confirmed by flow cytometry, and Western blot with *L. lactis* cell wall extract as previously described [19].

Immunisations

Vaccine aliquots were prepared as previously described, stored at –80ºC and enumerated after one freeze-thaw cycle. On immunisation days, an aliquot was thawed, washed and re-suspended in PBS. Animal work was performed at the Vernon Jansen Unit (VJU) at The University of Auckland and the Hercus-Taieri Resource Unit (HRTU) at The University of Otago under the guidelines and approvals of the University of Auckland Animal Ethics Committee and the University of Otago Animal Ethics Committee, respectively. Age and sex matched C57BL/6 mice (n = 5) were sourced from Jackson Laboratories (Bar Harbor, ME, USA, bred and housed in specific pathogen free conditions at the VJU or HRTU. Mice were immunised intranasally with recombinant *L. lactis* containing PilM1, PilM1-Ag85B$_{240–254}$, or PilM1-Ova$_{324–339}$ or s.c. with BCG under either aerosolised isoflurane anaesthesia or anaesthesia induced by intraperitoneal (i.p.) administration of 87 mg kg^{-1} ketamine (Phoenix Pharm Distributors, Auckland, New Zealand) and 2.6 mg kg^{-1} xylazine (Phoenix Pharm Distributors) in a 1:1 ratio. For delivery of the vaccines to the nasal mucosa, 1 x 10^8 CFU recombinant live *L. lactis* in a 5 μl volume were delivered under isoflurane anaesthesia on 3 consecutive days followed by three boosters 2 weeks apart (12 doses in total). Serum and samples from selected mucosal sites were obtained 2 weeks

after the final boost (day 58) as previously described. For delivery of the vaccines to the lower respiratory tract, 2 x10^7 CFU live recombinant *L. lactis* in a 40-µL volume were delivered under ketamine/xylazine anaesthesia for a total of three doses over 42 days. Lungs were collected two weeks following the final boost (day 48). BCG vaccination was delivered as 10^6 CFU in 200 µL subcutaneously on day 0, as previously described [44]. Serum was collected from the inferior *vena cava* prior to tissue dissection and processed as previously described[19].

Collection of samples from selected mucosal sites

Collection of serum samples, bronchoalveolar lavage (BAL) fluid and saliva samples were carried out as previously described [19]. Faecal samples were collected on day zero, and two weeks following the final boost (day 56). Faeces were weighed and suspended in PBS containing 1mM phenylmethylsulfononyl fluoride (PMSF, Sigma Aldrich) at a volume of 1mL per 100 mg of sample. Following homogenisation, samples were centrifuged at 10,000g for five minutes and the supernatant collected. Nasal washes were collected following bronchoalveolar lavage by holding the mouse ventrally and passing 1mL of PBS through the trachea and collecting as it passed through the nose.

ELISA

Microlon 96-well ELISA plates (Grenier Bio-One, Kremsmunster, Austria) were coated with 1 µg mL^{-1} recombinant Spy0128, commercial ovalbumin (Invivogen, Carlsbad, CA, USA) or commercial recombinant Ag85B (Abcam, Cambridge, UK) in PBS overnight at 4°C, or 1 µg mL^{-1} cognate peptide (GenScript, Piscataway, NJ, USA) in Carbonate-Bicarbonate buffer (pH 9.4) at 37 °C for 3 h. Plate were blocked with 3% BSA for 15 min prior to incubation with either titrated serum, BAL fluid, saliva, nasal or faecal samples. Goat anti-mouse IgG-HRP (Thermo Fisher Scientific, , Waltham, MA, USA) or goat anti-mouse IgA-HRP (Invitrogen) were used as secondary antibodies with 3,3,5,5-tetramethylbenzidine (Thermo Fisher Scientific) as the substrate. Absorbance was measured at OD450 nm using an EnSpire

multilabel plate reader (Perkin Elmer, Waltham, MA, USA). Endpoint titres were determined as the minimum serum dilution above the control (absorbance of 1:100 dilution of pre-immune serum, 1:5 pre-immune faecal samples, or background control wells plus 3 times the standard deviation). All ELISAs were carried out in duplicates.

Resident lung lymphocyte isolation

Lungs were perfused by injecting 1 mL of PBS into the right atrium of the heart before dissection. Lungs were cut into small pieces and incubated in incomplete Iscove's Modified Dulbecco's Medium (IMDM, Sigma Aldrich) supplemented with 2.4 mg mL^{-1} Collagenase I (Life Technologies) and 0.12 mg mL^{-1} DNase I (Roche) for 1 h at 37°C with 5% CO_2. Digested lungs were pushed gently through 70 µm nylon strainers to obtain single cell suspensions and counted using a haemocytometer after Trypan Blue staining.

Tetramer enrichment

Ag85B MHC class II Tetramer IAb/FQDAYNAAG GHNAVF was provided by the National Institute of Allergy and Infectious Disease Facility, Emory University, Atlanta, GA, USA. Microbead-based enrichment of tetramer positive cells was performed as previously described [45]. Briefly, lung cells were incubated with tetramer in FACS buffer (PBS + 1% FCS, 5 mM EDTA) and incubated at 37°C with 5% CO_2 for 30 minutes. Cells were washed, then resuspended in 90 µL enrichment buffer (FACS buffer + 2 mM EDTA, 20 µg mL^{-1} DNaseI (Roche, Basel, Switzerland) with 10% v/v anti-APC microbeads (Miltenyi Biotech, Bergisch Gladbach, Germany) and incubated for 15 minutes at 4ºC shielded from light. Cells were washed then microbead-bound cells were positively selected using an AutoMACS (Miltenyi Biotech). A pooled sample of lung cells from each group was stained with the control hCLIP tetramer to assess nonspecific staining. Cells were counted following enrichment using a haemocytometer and Trypan Blue staining.

455

456 **Cytokine stimulation**

457 Corning Costar® 24 well plates (Sigma-Aldrich) were seeded with 10^6 cells per well in 1 mL incomplete
458 IMDM (Thermo Fisher Scientific) and incubated with 20 μg $mL^{-1}$of cognate peptide at 37°C with 5%
459 CO_2 for 12 hours. Cells were incubated for a further six hours with 10 μg mL^{-1} Brefeldin A. After
460 incubation, cells were analysed by flow cytometry.

461

462 **Flow cytometry**

463 All staining was carried out at 4ºC shielded from light. Live/Dead staining and Fc-receptor blocking was
464 carried out prior to incubation with cell surface antibodies in FACS buffer. Cells enriched for specific
465 tetramer were stained with previously titrated antibodies specific for CD3, CD4, CD44, CD62L and
466 CD69 (Table 2). Cells stimulated with cognate peptide were stained with surface antibodies specific for
467 CD3, CD4 and CD8, and intracellular staining was carried out with antibodies specific for IL-2, IL-17,
468 IFN-γ and TNFα (Table 3) following incubation with saponin permeabilisation buffer. Analysis was
469 performed using a BD LSRFortessa (BD Biosciences) and analysed FlowJo (FlowJo, LLC, Ashland, OR,
470 USA). Gates were set using unstained and fluorescence-minus-one controls.

471

472 **Statistical analysis**

473 Statistical analysis was carried out using Prism (GraphPad). Data was tested for normal distribution and
474 variance prior to comparative analyses. Where these assumptions were met, *t*-tests were carried out for
475 comparison of two data sets, while one-way ANOVA using Tukey analysis was carried out for
476 comparison of three or more data sets. If normality and variance assumptions were not met and
477 transforming the data to its logarithmic values did not correct for this, non-parametric tests were carried
478 out. Mann-Whitney *U*-tests were used to compare two data sets while the Kruskall-Wallis test was used
479 to compare three or more data sets.

Conflicts of interest

The authors have no conflicts of interest to declare.

ACKNOWLEDGMENTS

This study was funded by a Marsden research grant from the Royal Society of New Zealand. S. Blanchett was a recipient of a University of Auckland doctoral scholarship. C Tsai is an Auckland Medical Research Foundation (AMRF) Postdoctoral Research Fellow. J Loh is a NZ National Heart Foundation Senior Research Fellow.

References

1. WHO. Global tuberculosis report 2019.
2. Furin J, Cox H, Pai M. Tuberculosis. *Lancet* 2019; **393**: 1642-1656.
3. (CDC) CfDCaP. The Costly Burden of DrugResistant TB Disease in the U.S.: Centers for Disease Control and Prevention (CDC); 2018.
4. Oettinger T, Jorgensen M, Ladefoged A, Haslov K, Andersen P. Development of the *Mycobacterium bovis* BCG vaccine: review of the historical and biochemical evidence for a genealogical tree. *Tuber Lung Dis* 1999; **79**: 243-250.
5. Ronan EO, Lee LN, Tchilian EZ, Beverley PCL. Nasal associated lymphoid tissue (NALT) contributes little to protection against aerosol challenge with *Mycobacterium tuberculosis* after immunisation with a recombinant adenoviral vaccine. *Vaccine* 2010; **28**: 5179-5184.
6. Fine PEM. Variation in protection by BCG: implications of and for heterologous immunity. *The Lancet* 1995; **346**: 1339-1345.
7. Andersen P, Doherty TM. The success and failure of BCG — implications for a novel tuberculosis vaccine. *Nat Rev Microbiol* 2005; **3**: 656-662.
8. Kirman JR, Henao-Tamayo MI, Agger EM. The Memory Immune Response to Tuberculosis. *Microbiol Spectr* 2016; **4**.
9. Desel C, Dorhoi A, Bandermann S, Grode L, Eisele B, Kaufmann SH. Recombinant BCG Δ*ureC hly*$^{+}$ induces superior protection over parental BCG by stimulating a balanced combination of type 1 and type 17 cytokine responses. *J Infect Dis* 2011; **204**: 1573-1584.
10. Saqib M, Khatri R, Singh B, Gupta A, Kumar A, Bhaskar S. *Mycobacterium indicus pranii* as a booster vaccine enhances BCG induced immunity and confers higher protection in animal models of tuberculosis. *Tuberculosis (Edinb)* 2016; **101**: 164-173.
11. Zhang L, Jiang Y, Cui Z*, et al. Mycobacterium vaccae* induces a strong T_h1 response that subsequently declines in C57BL/6 mice. *J Vet Sci* 2016; **17**: 505-513.

12. Steigler P, Verrall AJ, Kirman JR. Beyond memory T cells: mechanisms of protective immunity to tuberculosis infection. *Immunol Cell Biol* 2019; **97**: 647-655.
13. Kondratieva TK, Rubakova EI, Linge IA, Evstifeev VV, Majorov KB, Apt AS. B cells delay neutrophil migration toward the site of stimulus: tardiness critical for effective bacillus Calmette-Guérin vaccination against tuberculosis infection in mice. *J Immunol* 2010; **184**: 1227-1234.
14. Harth G, Lee BY, Wang J, Clemens DL, Horwitz MA. Novel insights into the genetics, biochemistry, and immunocytochemistry of the 30-kilodalton major extracellular protein of *Mycobacterium tuberculosis*. *Infect Immun* 1996; **64**: 3038-3047.
15. Karbalaei Zadeh Babaki M, Soleimanpour S, Rezaee SA. Antigen 85 complex as a powerful *Mycobacterium tuberculosis* immunogene: Biology, immune-pathogenicity, applications in diagnosis, and vaccine design. *Microb Pathog* 2017; **112**: 20-29.
16. Luabeya AKK, Kagina BMN, Tameris MD*, et al.* First-in-human trial of the post-exposure tuberculosis vaccine H56:IC31 in *Mycobacterium tuberculosis* infected and non-infected healthy adults. *Vaccine* 2015; **33**: 4130-4140.
17. Derrick SC, Kolibab K, Yang A, Morris SL. Intranasal administration of *Mycobacterium bovis* BCG induces superior protection against aerosol infection with *Mycobacterium tuberculosis* in mice. *Clin Vaccine Immunol* 2014; **21**: 1443-1451.
18. Giudice EL, Campbell JD. Needle-free vaccine delivery. *Advanced Drug Delivery Reviews* 2006; **58**: 68-89.
19. Wagachchi D, Tsai J-YC, Chalmers C, Blanchett S, Loh JMS, Proft T. PilVax - a novel peptide delivery platform for the development of mucosal vaccines. *Sci Rep* 2018; **8**: 2555-2555.
20. Mora M, Bensi G, Capo S*, et al.* Group A Streptococcus produce pilus-like structures containing protective antigens and Lancefield T antigens. *Proc Natl Acad Sci USA* 2005; **102**: 15641-15646.
21. Kang HJ, Coulibaly F, Clow F, Proft T, Baker EN. Stabilizing Isopeptide Bonds Revealed in Gram-Positive Bacterial Pilus Structure. *Science* 2007; **318**: 1625.

22. Linke C, Young PG, Kang HJ*, et al.* Crystal structure of the minor pilin FctB reveals determinants of Group A streptococcal pilus anchoring. *J Biol Chem* 2010; **285**: 20381-20389.
23. Kreikemeyer B, Nakata M, Oehmcke S, Gschwendtner C, Normann J, Podbielski A. Streptococcus pyogenes Collagen Type I-binding Cpa Surface Protein: EXPRESSION PROFILE, BINDING CHARACTERISTICS, BIOLOGICAL FUNCTIONS, AND POTENTIAL CLINICAL IMPACT. *J Biol Chem* 2005; **280**: 33228-33239.
24. Clow F, Peterken K, Pearson V, Proft T, Radcliff FJ. PilVax, a novel *Lactococcus lactis*-based mucosal vaccine platform, stimulates systemic and mucosal immune responses to *Staphylococcus aureus*. *Immunol Cell Biol* 2020; **98**: 369-381.
25. Kariyone A, Tamura T, Kano H*, et al.* Immunogenicity of Peptide-25 of Ag85B in T_h1 development: role of IFN-γ. *Int Immunol* 2003; **15**: 1183-1194.
26. Takatsu K, Kariyone A. The immunogenic peptide for T_h1 development. *Int Immunopharmacol* 2003; **3**: 783-800.
27. Song K, Bolton DL, Wei CJ*, et al.* Genetic immunization in the lung induces potent local and systemic immune responses. *Proc Natl Acad Sci USA* 2010; **107**: 22213-22218.
28. Linke-Winnebeck C, Paterson NG, Young PG*, et al.* Structural model for covalent adhesion of the *Streptococcus pyogenes* pilus through a thioester bond. *J Biol Chem* 2014; **289**: 177-189.
29. Bahey-El-Din M. *Lactococcus lactis*-based vaccines from laboratory bench to human use: an overview. *Vaccine* 2012; **30**: 685-690.
30. Vogelzang A, Perdomo C, Zedler U*, et al.* Central Memory $CD4^+$ T Cells Are Responsible for the Recombinant Bacillus Calmette-Guérin Δ*ureC::hly* Vaccine's Superior Protection Against Tuberculosis. *J Infect Dis* 2014; **210**: 1928-1937.
31. Woodworth JS, Christensen D, Cassidy JP, Agger EM, Mortensen R, Andersen P. Mucosal boosting of H56:CAF01 immunization promotes lung-localized T cells and an accelerated

pulmonary response to *Mycobacterium tuberculosis* infection without enhancing vaccine protection. *Muc Immunol* 2019; **12**: 816-826.

32. Lin PL, Dietrich J, Tan E*, et al.* The multistage vaccine H56 boosts the effects of BCG to protect cynomolgus macaques against active tuberculosis and reactivation of latent *Mycobacterium tuberculosis* infection. *J Clin Invest* 2012; **122**: 303-314.

33. Maurer MA, Meyer L, Bianchi M*, et al.* Glycosylation of Human IgA Directly Inhibits Influenza A and Other Sialic-Acid-Binding Viruses. *Cell Reports* 2018; **23**: 90-99.

34. Schroten H, Stapper C, Plogmann R, Kohler H, Hacker J, Hanisch FG. Fab-independent antiadhesion effects of secretory immunoglobulin A on S-fimbriated *Escherichia coli* are mediated by sialyloligosaccharides. *Infect Immun* 1998; **66**: 3971-3973.

35. Boren T, Falk P, Roth KA, Larson G, Normark S. Attachment of *Helicobacter pylori* to human gastric epithelium mediated by blood group antigens. *Science* 1993; **262**: 1892.

36. Chen T, Blanc C, Eder AZ*, et al.* Association of Human Antibodies to Arabinomannan With Enhanced Mycobacterial Opsonophagocytosis and Intracellular Growth Reduction. *J Infect Dis* 2016; **214**: 300-310.

37. Lambkin-Williams R, Gelder C, Broughton R*, et al.* An Intranasal Proteosome-Adjuvanted Trivalent Influenza Vaccine Is Safe, Immunogenic & Efficacious in the Human Viral Influenza Challenge Model. Serum IgG & Mucosal IgA Are Important Correlates of Protection against Illness Associated with Infection. *PLOS ONE* 2016; **11**: e0163089.

38. Perdomo C, Zedler U, Kühl AA*, et al.* Mucosal BCG Vaccination Induces Protective Lung-Resident Memory T Cell Populations against Tuberculosis. *mBio* 2016; **7**: e01686-01616.

39. Connor LM, Harvie MC, Rich FJ*, et al.* A key role for lung-resident memory lymphocytes in protective immune responses after BCG vaccination. *Eur J Immunol* 2010; **40**: 2482-2492.

40. Manrique M, Kozlowski PA, Wang SW*, et al.* Nasal DNA-MVA SIV vaccination provides more significant protection from progression to AIDS than a similar intramuscular vaccination. *Muc Immunol* 2009; **2**: 536-550.

41. Cowley SC, Hamilton E, Frelinger JA, Su J, Forman J, Elkins KL. $CD4^-CD8^-$ T cells control intracellular bacterial infections both in *vitro* and in *vivo*. *J Exp Med* 2005; **202**: 309-319.

42. Cowley SC, Meierovics AI, Frelinger JA, Iwakura Y, Elkins KL. Lung $CD4^-CD8^-$ double-negative T cells are prominent producers of IL-17A and IFN-γ during primary respiratory murine infection with *Francisella tularensis* live vaccine strain. *J Immunol* 2010; **184**: 5791-5801.

43. Masonou T, Hokey DA, Lahey T*, et al.* $CD4^+$ T cell cytokine responses to the DAR-901 booster vaccine in BCG-primed adults: a randomized, placebo-controlled trial. *PLOS ONE* 2019; **14**: e0217091.

44. Quinn KM, Rich FJ, Goldsack LM*, et al.* Accelerating the secondary immune response by inactivating $CD4^+CD25^+$ T regulatory cells prior to BCG vaccination does not enhance protection against tuberculosis. *Eur J Immunol* 2008; **38**: 695-705.

45. Ancelet LR, Aldwell FE, Rich FJ, Kirman JR. Oral vaccination with lipid-formulated BCG induces a long-lived, multifunctional $CD4^+$ T cell memory immune response. *PLoS One* 2012; **7**: e45888.

607 **Table 1.** Absolute number of DN T cells producing each cytokine (or combination) was generally higher

608 in *L. lactis* PilM1-Ag85B$_{240-254}$ vaccinated mice than BCG vaccinated mice

	Mean number of cells	
Cytokines produced	PilVax-Ag85B	BCG
IFN_γ	147	143
IL-2	133	204
TNFα	90	43
IL-17	427	170
IFN_γ, IL-2	1	5
IFN_γ, TNFα	4	2
IFN_γ IL-17	53	12
IL2, TNFα	2	3
IL-2, IL-17	5	10
IL17, TNFα	77	20
IFN_γ, IL-2, TNFα	0	0
IFN_γ, IL-2, IL-17	0	2
IFN_γ, TNFα, IL-17	5.85	5
IL-2, TNFα, IL-17	2.43	0
IFN_γ, IL-2, TNFα, IL-17	0	0

609

610

611

612 **Table 2.** Antibody panel: $CD4^+$ T cell identification

Specificity	Fluorophore	Clone	Supplier	Detector
CD3	FITC	17A2	BD PharMingen	Blue 530/30
CD4	BB700	RM4-5	BD Horizon	Blue 710/50
CD44	BV421	IM7	BD PharMingen	Violet 450/50
CD62L	BV510	MEL-14	BD Horizon	Violet 525/50
CD69	PE-CF594	H1.2F3	BD PharMingen	Green 610/20
Live/Dead	FSV700	-	BD Horizon	Red 730/45
FC block	-	-		
Ag85B MHC class II Tetramer IAb/FQDAYNAAG GHNAVF	APC	-	*	Red 670/14
ESAT-6_P1 MHC class II Tetramer IAb/QQWNFAGIE AAASA	APC	-	*	Red 670/14
hCLIP Tetramer	APC	-	*	Red 670/14

613

614

615 **Table 3.** Antibody panel: cytokine production identification

Specificity	Fluorophore	Clone	Supplier	Detector
CD3	FITC	17A2	BD PharMingen	Blue 530/30
CD4	BB700	RM4-5	BD Horizon	Blue 710/50
CD8	APC-cy7	53.67	BD PharMingen	Red 780/60
IL-2	APC	JE56 5HH	Biolegend	Red 670/14
IFN-γ	BV510	XM G1.2	BD PharMingen	Violet 585/15
TNFα	BV711	MP6.XT22	BD Biosciences	Violet 711
IL-17	BV650	TCII 18H 10.1	Biolegend	Violet 650
Live/Dead	FSV700	-	BD Horizon	Red 730/45
Fc Block	-	-		

616

617

Figure captions

Figure 1. Heterologous expression of the GAS pilus on the surface of *L. lactis* with the Ag85B$_{240-254}$ peptide from *Mtb* genetically engineered into the Spy0128 backbone pilus protein.

(a) Western blot analysis of *L. lactis* cell wall extracts probed with M1_Spy0128 (pilus backbone protein) specific antisera. **(b)** Flow cytometry histogram plot of WT *L. lactis*, *L. lactis* PilM1 (no peptide), and *L. lactis* PilM1-Ag85B$_{240-254}$ labelled with anti-M1_Spy0128. **(c)** Flow cytometry data plotted as mean fluorescence intensity (MFI) used to compare surface expression levels of M1_Spy0128.

Figure 2. Intranasal immunisation with *L. lactis* PilM1-Ag85B$_{240-254}$ induces systemic and mucosal antibody responses.

C57BL/6 mice (n = 5) were immunised intranasally in a single experiment with $1x10^8$ CFU live recombinant *L. lactis* PilM1-Ag85B$_{240-254}$ in low doses for delivery to the upper respiratory tract. The previously characterised *L. lactis* PilM1-Ova was used as a control group. Ig titres were measured by ELISA. **(a)** Mean serum anti-Spy0128 IgG /IgA titres. **(b)** Mean serum anti-peptide IgG/IgA. **(c)** Mean IgA titres from selected mucosal sites.

C57BL/6 mice (n = 5) were immunised intranasally in a single experiment with 2 x 10^7 CFU live recombinant *L. lactis* PilM1-Ag85B$_{240-254}$ in high doses for delivery to the lower respiratory tract or s.c. with BCG as a positive control. **(d)** Serum anti-peptide IgG and IgA titres are shown.

ELISAs were carried out in duplicates. Horizontal bars represent the median values.

Figure 3. Intranasal immunisation with *L. lactis* PilM1-Ag85B$_{240-254}$ induces peptide specific CD4$^+$ T cells.

Groups of C57BL/6 mice (n = 5) were immunised intranasally in a single experiment with 2 x 10^7 CFU 40 μL^{-1} live recombinant *L. lactis* PilM1-Ag85B$_{240-254}$ or *L. lactis* PilM1 in high doses for delivery to the

lower respiratory tract. A positive control group of C57BL/6 mice (n = 5) were vaccinated s.c. with BCG. Lymphocytes were isolated from the lungs and enriched with a tetramer specific for the Ag85B-$_{240-254}$ peptide. **(a)** Representative dot plots showing gating strategy to identify tetramer positive $CD4^+$ cells among singlet, live, $CD4^+$ lymphocytes. Gates were set using unstained and fluorescence minus one control. **(b)** Proportion of peptide specific $CD4^+$ T cells as percentage of total $CD4^+$, and absolute number of peptide specific $CD4^+$ T cells numerated from cell counts pre/post tetramer enrichment and flow cytometer data. A pooled sample of cells from all groups was enriched with the hCLIP tetramer to assess nonspecific binding. *$P < 0.05$ by way of Kruskal-Wallis test. **(c)** Phenotypic analysis of peptide specific $CD4^+$ cells as identified by Boolean gating analysis of the cell subset with antibodies specific for indicated cell surface markers. *$P < 0.05$ by way of Mann-Whitney *U*-test. ELISAs were carried out in duplicates. Horizontal bars represent the median values.

Figure 4. Intranasal immunisation with *L. lactis* PilM1-Ag85B-$_{240-254}$ alters pulmonary T cell subsets.

Pulmonary lymphocytes isolated from groups of C57BL/6 mice (n = 5) immunised intranasally in a single experiment with 2 x10^7 live recombinant *L. lactis* (large dose regimen for lower respiratory tract delivery), or s.c. with BCG, were incubated with cognate peptide for 12 hours, then a further 6-hour incubation with Brefelden A. **(a)** Representative dot plots showing gating strategy to identify $CD4^+$ or $CD8^+$ T cells among singlet, live, $CD3^+$ lymphocytes. Gates were set using unstained and fluorescence minus one controls. **(b)** Proportion of $CD4^+$, $CD8^+$ and $CD4^-CD8^-$ $CD3^+$ T cells identified for each vaccination group.

Figure 5. Intranasal immunisation with *L. lactis* PilM1-Ag85B-$_{240-254}$ results in peptide specific IFN-γ and IL-17 production.

667 Representative dot plots showing gating strategy to identify intracellular IL-2, IL-17, TNFα and IFN-γ
668 production among re-stimulated pulmonary T cells subsets isolated from groups of C57BL/6 mice (n = 5)
669 immunised intranasally with 2 x10^7 live recombinant *L. lactis*, or s.c. with BCG in a single experiment.
670 Gates were set using unstained and fluorescence minus one control.
671
672 **Figure 6 Quantification of cytokine production**
673 Cytokine production was quantified from each T cell subset identified in figure 4**a**. Data points represent
674 responses from individual mice, with the line representing the mean % of cells producing a single
675 cytokine, or combination of cytokines. **(a)** $CD4^+$ T cells. **(b)** $CD8^+$ T cells. **(c)** $CD3^+$ $CD4^-$ $CD8^-$ T cells.

Figure 1

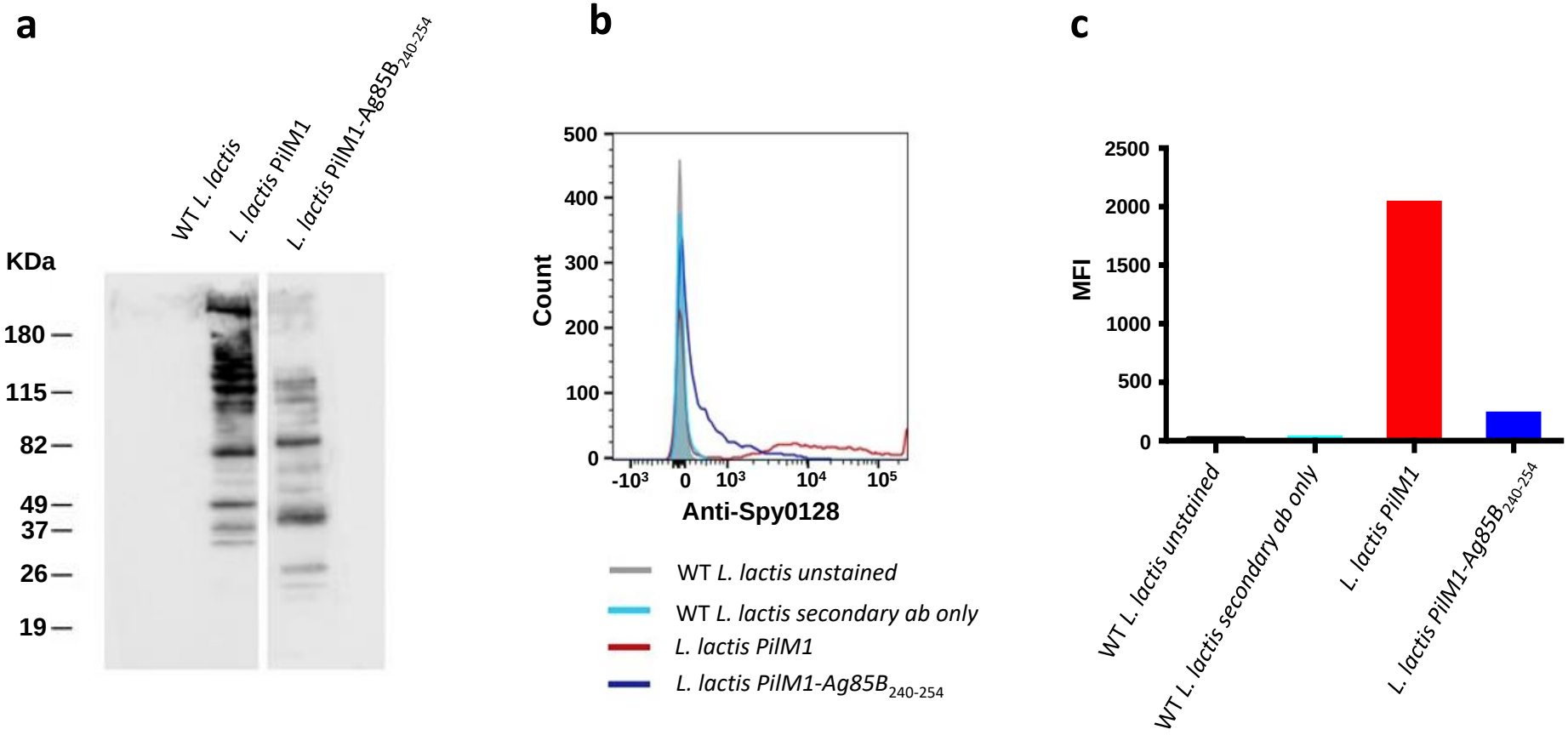
a
WT L. lactis
L. lactis PilM1
L. lactis PilM1-Ag85B240-254
KDa
180
115
82
49
37
26
19
b
Count
500
400
300
200
100
0
-10³
0
10³
10⁴
10⁵
Anti-Spy0128
WT L. lactis unstained
WT L. lactis secondary ab only
L. lactis PilM1
L. lactis PilM1-Ag85B240-254
c
MFI
2500
2000
1500
1000
500
0
WT L. lactis unstained
WT L. lactis secondary ab only
L. lactis PilM1
L. lactis PilM1-Ag85B240-254

Figure 2

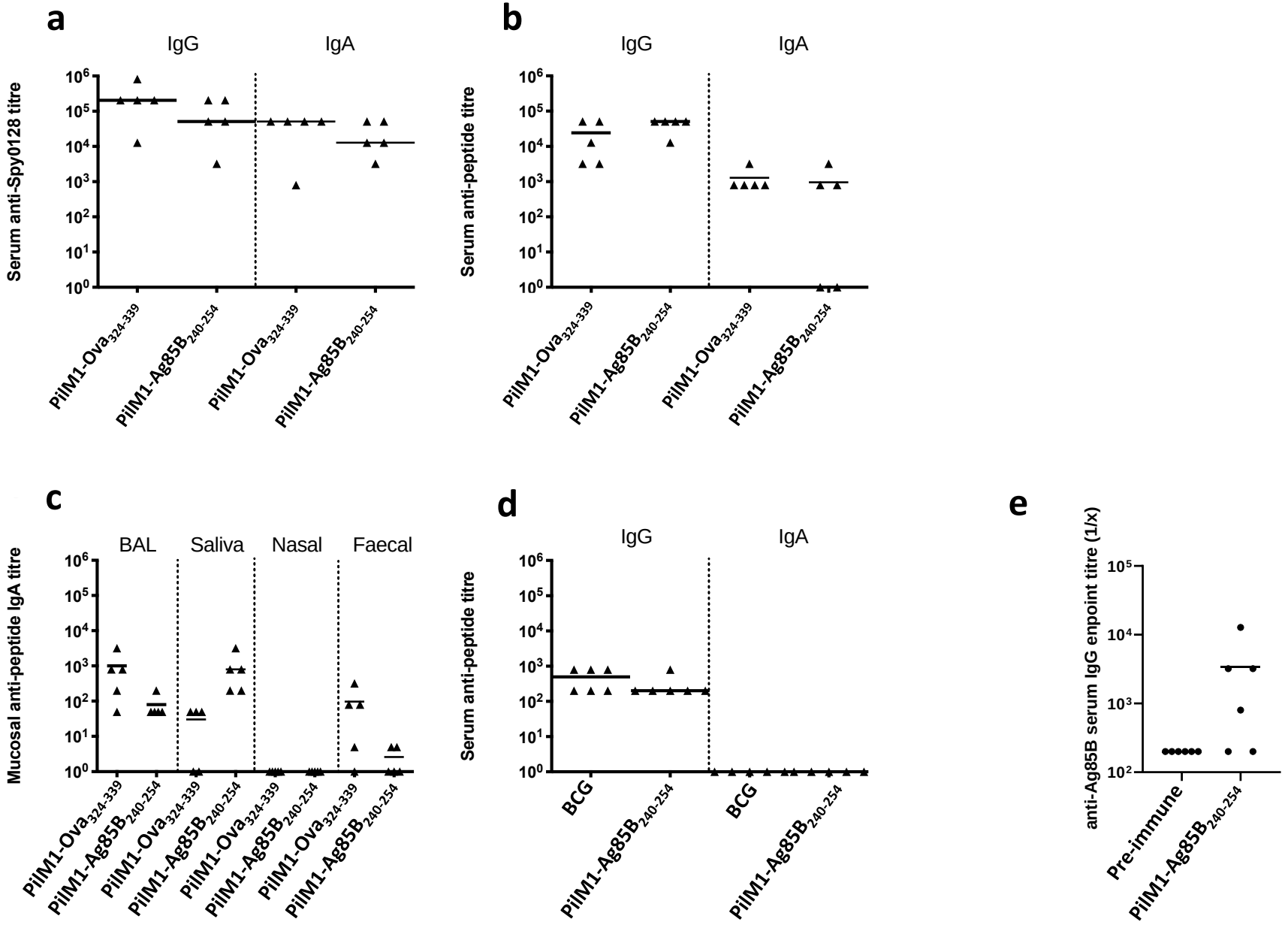
a
IgG
IgA
Serum anti-Spy0128 titre
PilM1-Ova324-339
PilM1-Ag85B240-254
PilM1-Ova324-339
PilM1-Ag85B240-254
b
IgG
IgA
Serum anti-peptide titre
PilM1-Ova324-339
PilM1-Ag85B240-254
PilM1-Ova324-339
PilM1-Ag85B240-254
c
BAL
Saliva
Nasal
Faecal
Mucosal anti-peptide IgA titre
PilM1-Ova324-339
PilM1-Ag85B240-254
PilM1-Ova324-339
PilM1-Ag85B240-254
PilM1-Ova324-339
PilM1-Ag85B240-254
PilM1-Ova324-339
PilM1-Ag85B240-254
d
IgG
IgA
Serum anti-peptide titre
BCG
PilM1-Ag85B240-254
BCG
PilM1-Ag85B240-254
e
anti-Ag85B serum IgG enpoint titre (1/x)
Pre-immune
PilM1-Ag85B240-254

Figure 3

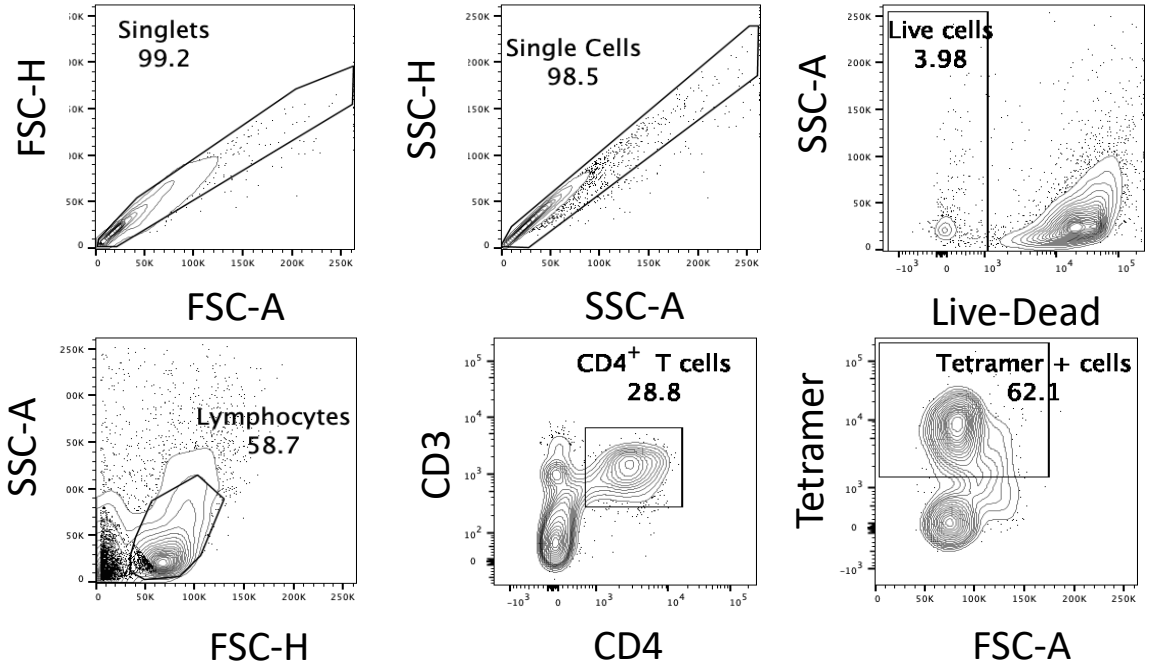
a
Singlets
99.2
FSC-H
FSC-A
Single Cells
98.5
SSC-H
SSC-A
Live cells
3.98
SSC-A
Live-Dead
Lymphocytes
58.7
SSC-A
FSC-H
CD4+ T cells
28.8
CD3
CD4
Tetramer + cells
62.1
Tetramer
FSC-A

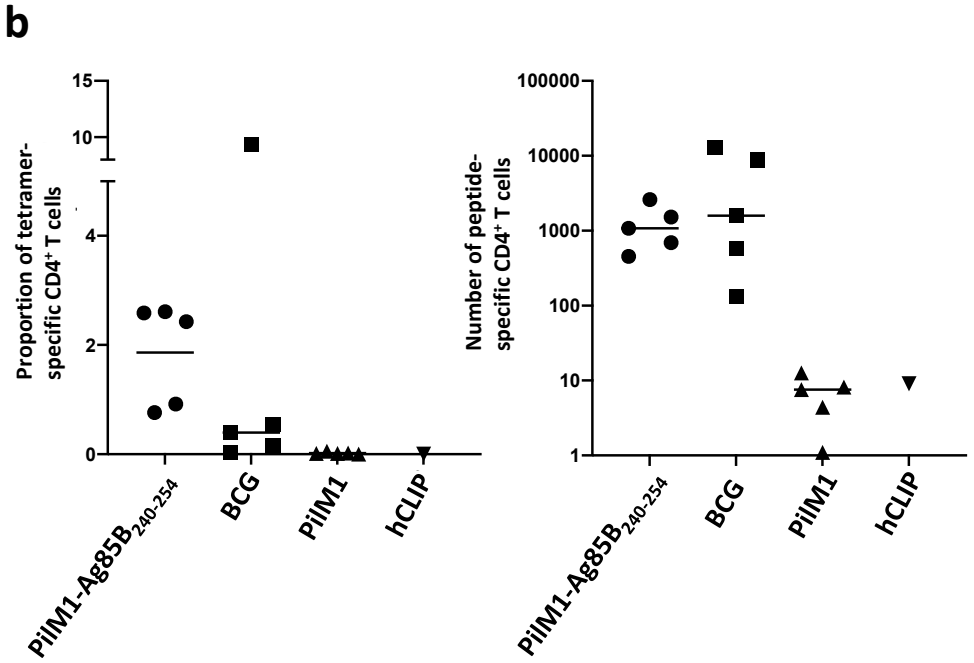
b
Proportion of tetramer-specific CD4+ T cells
Number of peptide-specific CD4+ T cells
PilM1-Ag85B240-254
BCG
PilM1
hCLIP

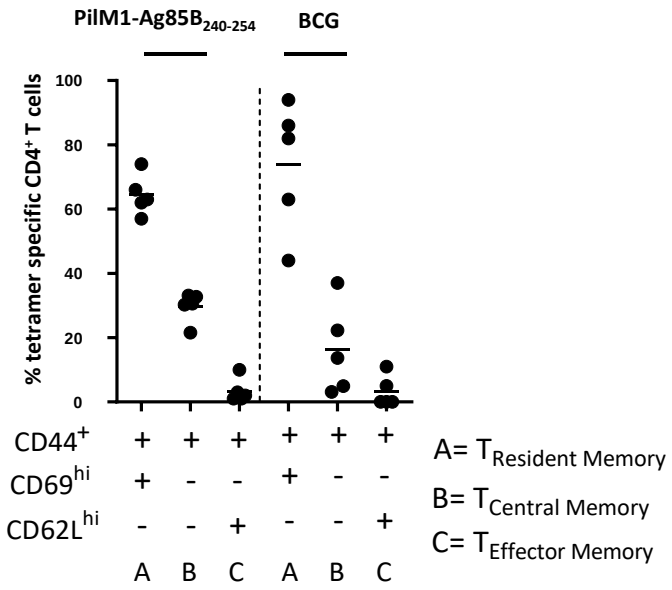
c
PilM1-Ag85B240-254
BCG
% tetramer specific CD4+ T cells
CD44+
CD69hi
CD62Lhi
A B C A B C
A= TResident Memory
B= TCentral Memory
C= TEffector Memory

Figure 4

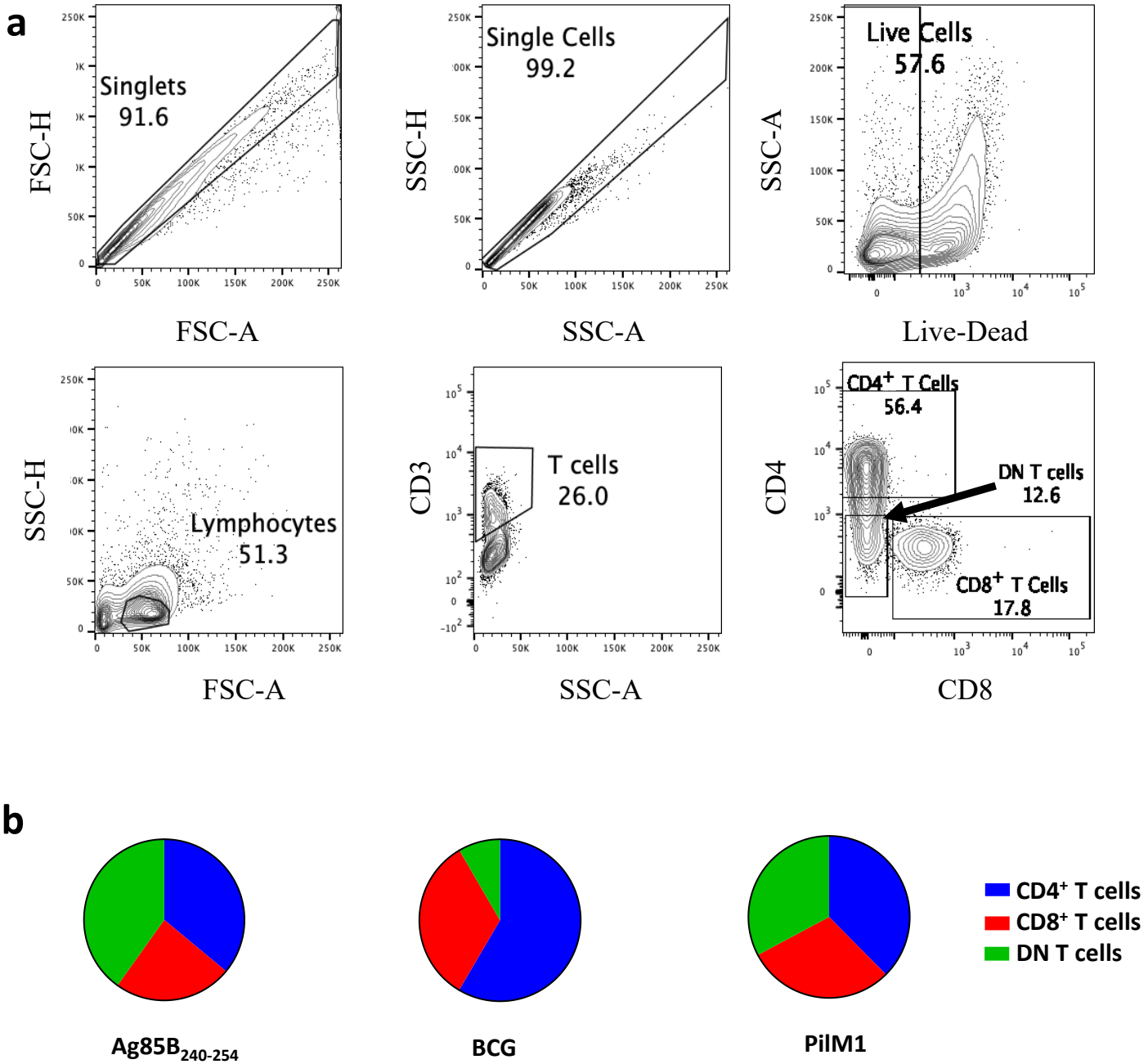
a
Singlets
91.6
FSC-H
FSC-A
Single Cells
99.2
SSC-H
SSC-A
Live Cells
57.6
SSC-A
Live-Dead
Lymphocytes
51.3
SSC-H
FSC-A
T cells
26.0
CD3
SSC-A
CD4+ T Cells
56.4
DN T cells
12.6
CD8+ T Cells
17.8
CD4
CD8
b
Ag85B240-254
BCG
PilM1
CD4+ T cells
CD8+ T cells
DN T cells

Figure 5

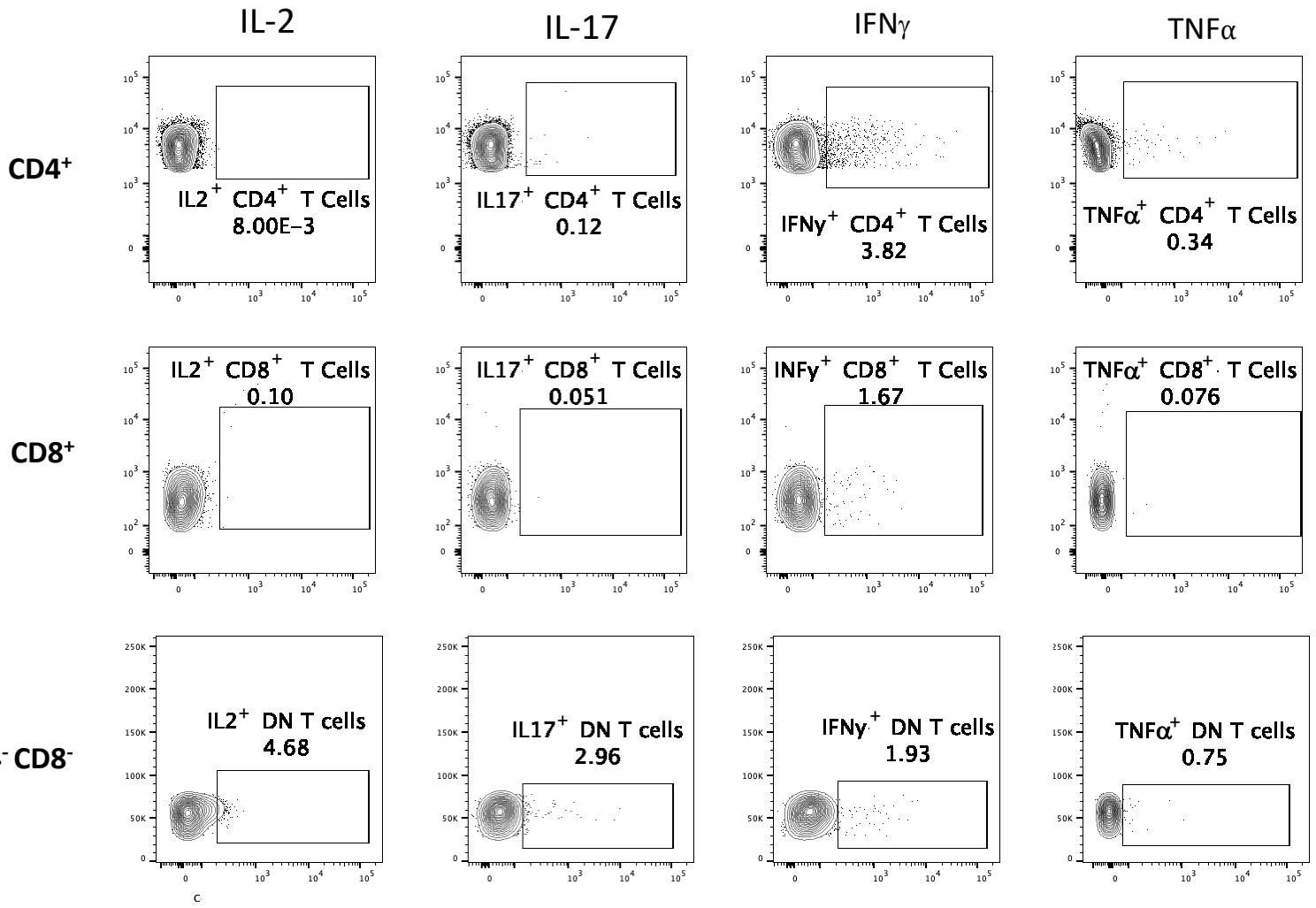
IL-2
IL-17
IFNγ
TNFα
CD4+
IL2+ CD4+ T Cells
8.00E−3
IL17+ CD4+ T Cells
0.12
IFNy+ CD4+ T Cells
3.82
TNFα+ CD4+ T Cells
0.34
CD8+
IL2+ CD8+ T Cells
0.10
IL17+ CD8+ T Cells
0.051
INFy+ CD8+ T Cells
1.67
TNFα+ CD8+ T Cells
0.076
CD4- CD8-
IL2+ DN T cells
4.68
IL17+ DN T cells
2.96
IFNy+ DN T cells
1.93
TNFα+ DN T cells
0.75

Figure 6

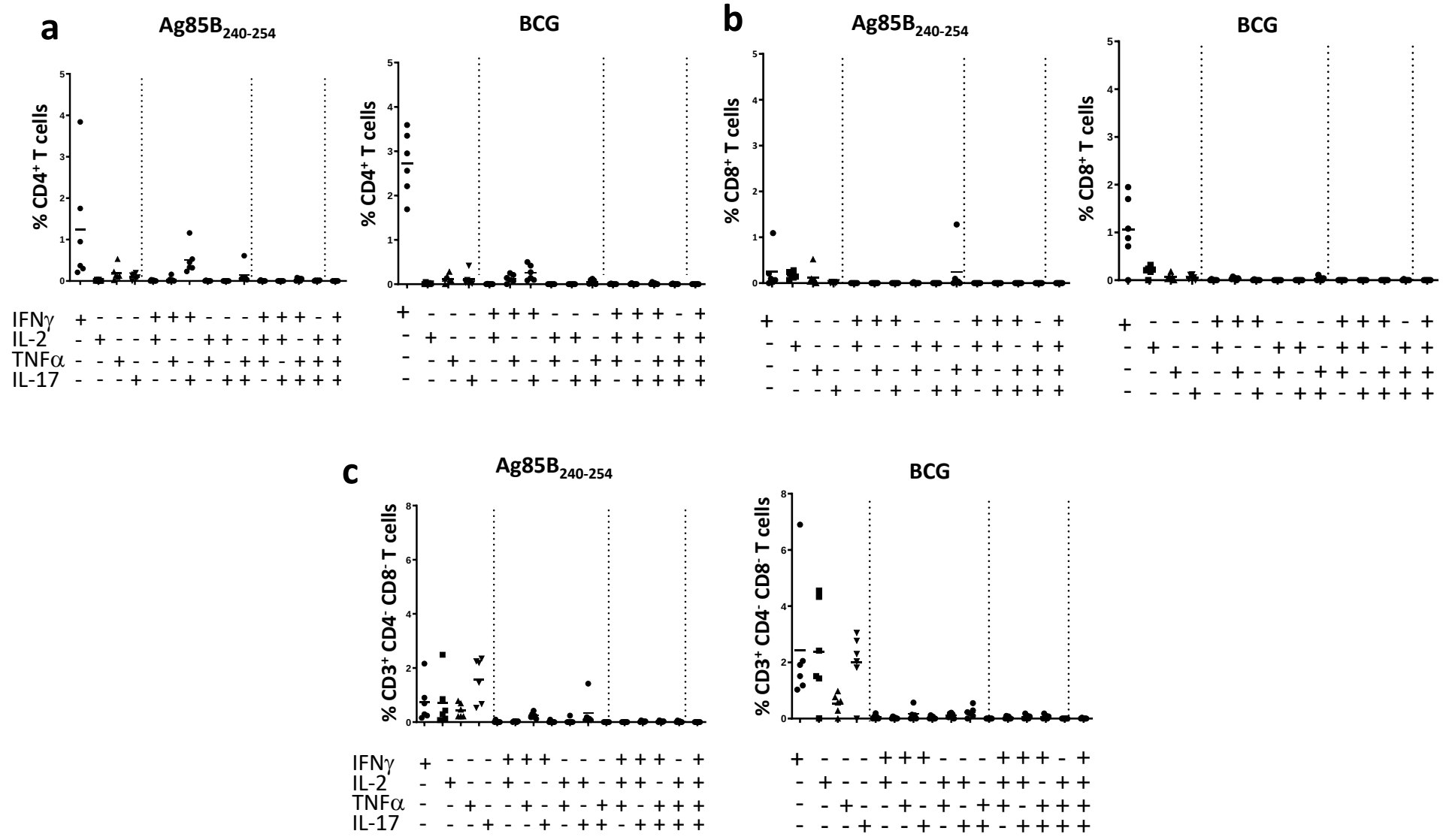
a
Ag85B240-254
BCG
% CD4+ T cells
b
% CD8+ T cells
c
% CD3+ CD4- CD8- T cells
IFNγ
IL-2
TNFα
IL-17